Strong-coupling expansions for the pure and disordered Bose-Hubbard model

J. K. Freericks
Department of Physics, Georgetown University, Washington, D.C. 20057

H. Monien
Theoretische Physik, Eidgenössische Technische Hochschule Hönggerberg, CH-8093 Zürich, Switzerland
(Received 23 August 1995)

A strong-coupling expansion for the phase boundary of the (incompressible) Mott insulator is presented for the Bose-Hubbard model. Both the pure case and the disordered case are examined. Extrapolations of the series expansions provide results that are as accurate as the Monte Carlo simulations and agree with the exact solutions. The shape difference between Kosterlitz-Thouless critical behavior in one-dimension and power-law singularities in higher dimensions arises naturally in this strong-coupling expansion. Bounded disorder distributions produce a ''first-order'' kink to the Mott phase boundary in the thermodynamic limit because of the presence of Lifshitz's rare regions.

I. INTRODUCTION

Strongly interacting bosonic systems have attracted a lot of recent interest.[1–4] Physical realizations include short-correlation-length superconductors, granular superconductors, Josephson arrays, the dynamics of flux lattices in type-II superconductors, and critical behavior of ^{4}He in porous media. The bosonic systems are either tightly bound composites of fermions that act like effective bosonic particles with soft cores or correspond to bosonic excitations that have repulsive interactions. For this reason, these systems are modeled by soft-core bosons which are described most simply by the Bose Hubbard model. Various aspects of this model were investigated analytically by mean-field theory,[1,5] by renormalization group techniques,[1,3] and by projection methods.[6] The Bose Hubbard model has also been studied with quantum Monte Carlo (QMC) methods by Scalettar and co-workers[2] in one dimension (1+1) and by Krauth and Trivedi,[7] van Otterlo and Wagenblast,[8] and Batrouni *et al.*[9] in two dimensions (2+1). In this contribution, the Mott-phase diagram is obtained from a strong-coupling expansion that has the correct dependence on spatial dimensionality, is as accurate as the QMC calculations, and agrees with the known exact solutions. Preliminary results for the pure case have already appeared.[10]

The Bose Hubbard model is the minimal model which contains the key physics of the strongly interacting Bose systems—the competition between kinetic and potential energy effects. Its Hamiltonian is

$$H=-\sum_{ij} t_{ij} b_i^\dagger b_j+\sum_i \epsilon_i \hat{n}_i-\mu\sum_i \hat{n}_i + \frac{1}{2}U\sum_i \hat{n}_i(\hat{n}_i-1), \quad \hat{n}_i=b_i^\dagger b_i, \tag{1}$$

where b_i is the boson annihilation operator at site i, t_{ij} is the hopping matrix element between the site i and j, ϵ_i is the local site energy, U is the strength of the on-site repulsion, and μ is the chemical potential. The hopping matrix is assumed to be a real symmetric matrix ($t_{ij}=t_{ji}$) and the lattice is also assumed to be bipartite; i.e., the lattice may be separated into two sublattices (the A sublattice and the B sublattice) such that t_{ij} vanishes whenever i and j both belong to the same sublattice (in particular, this implies $t_{ii}=0$). The local site energy ϵ_i is a quenched random variable chosen from a distribution of site energies that is symmetric about zero and satisfies $\Sigma_i \epsilon_i=0$. The pure case corresponds to all site energies vanishing ($\epsilon_i=0$).

The form of the zero-temperature ($T=0$) phase diagram can be understood by starting from the strong-coupling or ''atomic'' limit.[1,11,12] In this limit, the kinetic energy vanishes ($t_{ij}=0$) and every site is occupied by a fixed number of bosons, n_0. In the pure case, the ground-state boson occupancy (n_0) is the same for each lattice site, and is chosen to minimize the on-site energy. If the chemical potential $\mu=(n_0+\delta)U$ is parametrized in terms of the deviation δ from integer filling n_0, then the on-site energy is $E(n_0)=-\delta U n_0-\frac{1}{2}Un_0(n_0+1)$, and the energy to add a boson onto a particular site satisfies $E(n_0+1)-E(n_0)=-\delta U$. Thus for a nonzero δ, a finite amount of energy is required to move a particle through the lattice. The bosons are incompressible and localized, which produces a Mott insulator. For $\delta=0$, the ground-state energies of the two different boson densities are degenerate $[E(n_0)=E(n_0+1)]$ and no energy is needed to add or extract a particle; i.e., the compressibility is finite and the system is a conductor. As the strength of the hopping matrix elements increases, the range of the chemical potential μ about which the system is incompressible decreases. The Mott-insulator phase will completely disappear at a critical value of the hopping matrix elements. Beyond this critical value of t_{ij} the system is a superfluid.

In the disordered case, a Mott-insulating phase may or may not exist depending upon the strength of the disorder. The energy to add a boson onto site i becomes $E(n_0+1)-E(n_0)=\epsilon_i-\delta U$, so that the system is compressible if a site i can be found which satisfies $\epsilon_i=\delta U$. If the disorder is assumed to be symmetrically bounded about zero

($|\epsilon_i| \leqslant \Delta U$), then a Mott-insulator exists whenever $\Delta < 1/2$. The ground-state boson occupancy is uniformly equal to n_0 within the Mott-insulating phase which extends from $-\Delta \geqslant \delta \geqslant \Delta - 1$ (when $t_{ij}=0$). Once again, the bosons are incompressible within the Mott phase and the system is insulating. As the hopping matrix elements increase in magnitude, the range of the chemical potential within which the system is incompressible decreases until the Mott phase vanishes at a critical value of the hopping matrix elements. The compressible phase will typically also be an insulator and is called a Bose glass,[1] but it has been conjectured that in some cases the transition proceeds directly from the Mott insulator to the superfluid.[1,3]

The phase boundary between the incompressible phase (Mott insulator) and the compressible phase (superfluid or Bose glass) is determined here in a strong-coupling expansion by calculating both the energy of the Mott insulator and of a defect state (which contains an extra hole or particle) in a perturbative expansion of the single-particle terms, $-\Sigma_{ij} t_{ij} b_i^\dagger b_j + \Sigma_i \epsilon_i \hat{n}_i$. At the point where the energy of the Mott state is degenerate with the defect state, the system becomes compressible. In the pure case, the compressible phase is also superfluid, but in the disordered case, the compressible phase is a Bose glass (except possibly at the tip of the Mott lobe).[1,3]

There are two distinct cases for the defect state: $\delta < 0$ corresponds to adding a *particle* to the Mott-insulator phase (with n_0 bosons per site), and $\delta > 0$ corresponds to adding a *hole* to the Mott-insulator phase (with n_0+1) bosons per site. Of course, the phase boundary depends upon the number of bosons per site, n_0, of the Mott insulator phase.

To zeroth order in t_{ij}/U the Mott-insulating state is given by

$$|\Psi_{\rm Mott}(n_0)\rangle^{(0)} = \prod_{i=1}^{N} \frac{1}{\sqrt{n_0!}} (b_i^\dagger)^{n_0} |0\rangle, \tag{2}$$

where n_0 is the number of bosons on each site, N is the number of sites in the lattice, and $|0\rangle$ is the vacuum state. The defect state is characterized by one additional particle (hole) which moves coherently throughout the lattice. To zeroth order in the single-particle terms the wave function for the ''defect'' state is determined by degenerate perturbation theory:

$$|\Psi_{\rm def}(n_0)\rangle^{(0)}_{\rm part} = \frac{1}{\sqrt{n_0+1}} \sum_i f_i^{(\rm part)} b_i^\dagger |\Psi_{\rm Mott}(n_0)\rangle^{(0)},$$

$$|\Psi_{\rm def}(n_0)\rangle^{(0)}_{\rm hole} = \frac{1}{\sqrt{n_0}} \sum_i f_i^{(\rm hole)} b_i |\Psi_{\rm Mott}(n_0)\rangle^{(0)}, \tag{3}$$

where the f_i is the eigenvector of the corresponding single-particle matrix $S_{ij}^{(\rm part)}(n_0) \equiv -t_{ij} + \delta_{ij}\epsilon_i/(n_0+1)$ [$S_{ij}^{(\rm hole)}(n_0) \equiv -t_{ij} - \delta_{ij}\epsilon_i/n_0$] with the lowest eigenvalue (the hopping matrix is assumed to have a nondegenerate lowest eigenvalue). It is well known that the minimal eigenvalue of the single-particle matrix S_{ij} is larger than the sum of the minimal eigenvalue of the hopping matrix plus the minimal eigenvalue of the disorder matrix. However, it has been demonstrated that as the system size becomes larger and larger, the minimal eigenvalue approaches the sum of the minimal eigenvalues of the hopping matrix and of the disorder matrix as closely as desired[13] (because of the existence of arbitrarily large ''rare regions'' where the system looks pure with $\epsilon_i = -\Delta U$ or with $\epsilon_i = \Delta U$). Therefore, in the thermodynamic limit, the perturbative energy of each defect state becomes

$$E_{\rm def}^{(\rm part)}(n_0) - E_{\rm Mott}(n_0) = -\delta^{(\rm part)} U + \lambda_{\rm min}(n_0+1) - \Delta U + \cdots, \tag{4}$$

$$E_{\rm def}^{(\rm hole)}(n_0) - E_{\rm Mott}(n_0) = \delta^{(\rm hole)} U + \lambda_{\rm min} n_0 - \Delta U + \cdots, \tag{5}$$

to first order in S, where $\lambda_{\rm min}$ is the minimal eigenvalue of the hopping matrix $-t_{ij}$. In the case of nearest-neighbor hopping on a hypercubic lattice in d dimensions, the number of nearest neighbors satisfies $z=2d$ and the minimal eigenvalue is $\lambda_{\rm min} = -zt$.

The boundary between the incompressible phase and the compressible phase is determined when the energy difference between the Mott insulator and the defect state vanishes (the compressibility is assumed to approach zero continuously at the phase boundary). Thus two branches of the Mott lobe can be found depending upon whether the defect state is an additional hole or an additional particle. The two branches of the Mott-phase boundary meet when

$$\delta^{(\rm part)}(n_0) + 1 = \delta^{(\rm hole)}(n_0). \tag{6}$$

The additional one on the left hand side arises because δ is measured from the point $\mu/U = n_0$. Equation (6) may be used to estimate the critical value of the hopping matrix element beyond which no Mott-insulator phase exists. Let x denote the combination dt/U and consider the first-order expansions in Eqs. (4) and (5). The critical value of x satisfies

$$x_{\rm crit}(n_0) = \frac{1-2\Delta}{2(2n_0+1)}, \tag{7}$$

which vanishes when the disorder strength becomes too large ($\Delta \geqslant 1/2$). Note that the critical value of x is *independent* of the dimension of the lattice; *the dimensionality first enters at second order in t*. The slopes of the phase boundaries about the point $\mu = n_0 U$ are equal in magnitude [$\lim_{x\to 0}(d/dx)\,\delta^{(\rm part)}(n_0,x) = -\lim_{x\to 0}(d/dx)\,\delta^{(\rm hole)}(n_0+1,x)$], but change their magnitude as a function of the density n_0, *implying that the Mott-phase lobes always have an asymmetrical shape*. Note further that the presence of disorder shifts the phase boundaries uniformly by Δ, but the slope is *independent* of the disorder distribution.

The Bose Hubbard model in the absence of disorder is examined by a strong-coupling expansion through third order in the single-particle matrix S in Sec. II. The exact solution for an infinite-dimensional lattice[1] is examined and various different extrapolation techniques are employed that do and do not utilize additional information of the scaling analysis of the critical point. Section III describes the similar results

for the disordered Bose Hubbard model and a discussion follows in Sec. IV.

II. PURE CASE

The Bose Hubbard model in Eq. (1) is studied in the absence of disorder ($\epsilon_i=0$). The many-body version of Rayleigh-Schrödinger perturbation theory is employed throughout. To third order in t_{ij}/U, the energy of the Mott state with n_0 bosons per site becomes

$$E_{\rm Mott}(n_0)=N\Bigg[-\delta U n_0-\frac{1}{2}Un_0(n_0+1)-\frac{1}{N}\sum_{ij}\frac{t_{ij}^2}{U}n_0(n_0+1)\Bigg], \tag{8}$$

which is proportional to the number of lattice sites, N. Note that the odd-order terms in t_{ij}/U vanish in the above expansion (odd-order terms may enter for nonbipartite lattices). The energy difference between the Mott insulator and the defect state with an additional particle ($\delta<0$) satisfies

$$E_{\rm def}^{(\rm part)}(n_0)-E_{\rm Mott}(n_0)=-\delta^{(\rm part)}U+\lambda_{\rm min}(n_0+1)+\frac{1}{2U}\sum_{ij}t_{ij}^2f_j^2n_0(5n_0+4)-\frac{1}{U}\lambda_{\rm min}^2n_0(n_0+1)$$
$$+\frac{1}{U^2}n_0(n_0+1)\Bigg[(2n_0+1)\lambda_{\rm min}^3-\left(\frac{25}{4}n_0+\frac{7}{2}\right)\lambda_{\rm min}\sum_{ij}t_{ij}^2f_j^2-(4n_0+2)\sum_{ij}f_it_{ij}^3f_j\Bigg], \tag{9}$$

to third order in t_{ij}/U, while the energy difference between the Mott-insulating phase and the defect phase with an additional hole ($\delta>0$) satisfies

$$E_{\rm def}^{(\rm hole)}(n_0)-E_{\rm Mott}(n_0)=\delta^{(\rm hole)}U+\lambda_{\rm min}n_0+\frac{1}{2U}\sum_{ij}t_{ij}^2f_j^2(n_0+1)(5n_0+1)-\frac{1}{U}\lambda_{\rm min}^2n_0(n_0+1)$$
$$+\frac{1}{U^2}n_0(n_0+1)\Bigg[(2n_0+1)\lambda_{\rm min}^3-\left(\frac{25}{4}n_0+\frac{11}{4}\right)\lambda_{\rm min}\sum_{ij}t_{ij}^2f_j^2-(4n_0+2)\sum_{ij}f_it_{ij}^3f_j\Bigg]. \tag{10}$$

The eigenvector f_i is the minimal eigenvector of the hopping matrix $-t_{ij}$ with eigenvalue $\lambda_{\rm min}$ and is identical in the particle and hole sectors. These results have been verified by small-cluster calculations on two- and four-site clusters. Note that the energy difference in Eqs. (9) and (10) is *independent* of the lattice size N, indicating that QMC simulations should not have a very strong dependence on the lattice size.

In the case of nearest-neighbor hopping on a d-dimensional hypercubic lattice, the minimum eigenvalue satisfies $\lambda_{\rm min}=-zt$, the sum $\Sigma_{ij}t_{ij}^2f_j^2$ becomes zt^2, and the sum $\Sigma_{ij}f_it_{ij}^3f_j$ equals zt^3. Equations (9) and (10) can then be solved for the shift in the chemical potential δ at which the system becomes compressible as a function of the parameter $x\equiv dt/U$. The results for the upper boundary are given by

$$\delta^{(\rm part)}(n_0,x)=-2x(n_0+1)+\frac{1}{d}x^2n_0(5n_0+4)-4x^2n_0(n_0+1)+2x^3n_0(n_0+1)\Bigg[\left(-8+\frac{25}{2d}-\frac{4}{d^2}\right)n_0+\left(-4+\frac{7}{d}-\frac{2}{d^2}\right)\Bigg], \tag{11}$$

to third order in x, and the lower boundary is given by

$$\delta^{(\rm hole)}(n_0,x)=2xn_0-\frac{1}{d}x^2(n_0+1)(5n_0+1)+4x^2n_0(n_0+1)-2x^3n_0(n_0+1)\Bigg[\left(-8+\frac{25}{2d}-\frac{4}{d^2}\right)n_0+\left(-4+\frac{11}{2d}-\frac{2}{d^2}\right)\Bigg], \tag{12}$$

to third order in x.

As a further check on the accuracy of the Mott-phase boundaries in Eqs. (11) and (12), we compare the perturbative expansion to the exact solution on an infinite-dimensional hypercubic lattice[1] (which corresponds to the mean-field solution). Note that the solution in Ref. 1 was for the infinite-range-hopping model; this solution is *identical* to that on an infinite-dimensional lattice in the pure case. The Mott-phase boundary may be expressed as

$$\frac{\mu}{U}-n_0=-\frac{1}{2}-x\pm\sqrt{x^2-x(2n_0+1)+\frac{1}{4}}, \tag{13}$$

where the plus sign denotes the upper branch to the Mott lobe ($\delta^{(\rm part)}$), and the minus sign corresponds to the lower

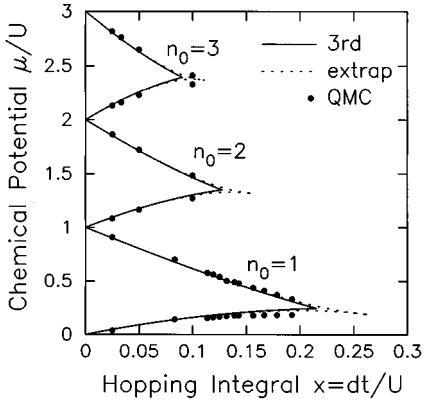

FIG. 1. The x, μ phase diagram of the Bose Hubbard model in one dimension ($d=1$). The solid lines give the phase boundaries of the Mott insulator to the superfluid state as determined from a third-order strong-coupling calculation. The dotted line is the constrained fit to a Kosterlitz-Thouless form. The circles are the result of the QMC calculation of Scalettar and co-workers (Ref. 2).

branch ($\delta^{(\mathrm{hole})}-1$). The critical point can also be determined as the value of x where the square root vanishes. One finds

$$x_{\mathrm{crit}}=n_0+\frac{1}{2}-\sqrt{n_0(n_0+1)}, \tag{14}$$

which depends on n_0 as $1/n_0$ in the limit of large n_0. The strong-coupling expansions (11) and (12) agree with the exact solution (13) when the latter is expanded out to third order in x, providing an independent check of the algebra. Note further that the exact solution uniquely determines the expansion coefficients of the powers of x that do not involve inverse powers of d and the perturbation expansion is only required to determine the $1/d$ corrections.

The strong-coupling expansion for the x, μ phase diagram in one dimension is compared to the QMC results of Scalettar and co-workers[2] in Fig. 1. The solid lines indicate the phase boundary between the Mott-insulator phase and the superfluid phase at zero temperature as calculated from Eq. (11) and Eq. (12). The solid circles are the results of the QMC calculation[2] at a small but finite temperature ($T\approx U/2$). The dotted line is an extrapolation from the series calculation that will be described below. Note that the overall agreement of the two calculations is excellent. For example, the critical value of the hopping matrix element for the first Mott lobe (n_0) is $x_{\mathrm{crit}}=0.215$, while the QMC calculations found[2] $x_{\mathrm{crit}}=0.215\pm0.01$. A closer examination of Fig. 1 shows a systematic deviation of the lower branch for larger values of x. We believe that this is most likely a finite-temperature effect, since the Mott-insulator phase becomes more stable at higher temperatures,[5] and the systematic errors of the QMC calculation due to finite lattice size and finite Trotter error are easily controlled.[14]

It is known from the scaling theory of Fisher *et al.*[1] that the phase transition at the tip of the Mott lobe is in the universality class of the $(d+1)$-dimensional XY model. Although a finite-order perturbation theory cannot describe the physics of the tricritical point correctly, we find that the density fluctuations dominate the physics of the phase transition even close to the tricritical point. Note how the Mott lobes have a cusplike structure in one dimension, mimicking the Kosterlitz-Thouless behavior of the critical point.

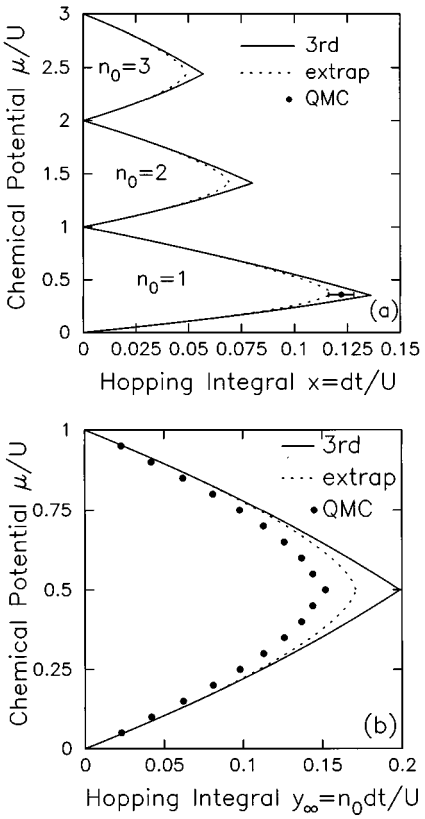

FIG. 2. (a) The x, μ phase diagram of the Bose Hubbard model in two dimensions ($d=2$). The solid lines give the phase boundaries of the Mott insulator to the superfluid state as determined from a third-order strong-coupling calculation. The dotted line is the constrained fit to a power-law form with exponent $z\nu=2/3$. The point (with error bars) indicates the tricritical point as determined by the QMC calculation of Krauth and Trivedi (Ref. 7) (no value for μ_{crit} was given in Ref. 7). (b) The y_∞, μ phase diagram for the quantum rotor model in two dimensions. The solid lines are the perturbative results to third order and the dotted lines are the constrained extrapolation fit. The dots are the QMC results of van Otterlo and Wagenblast (Ref. 8). The disagreement between the QMC and the extrapolated results most likely arises from the use of the Villain approximation in the former.

Figure 2(a) presents the strong-coupling expansion for the x, μ phase diagram in two dimensions. For comparison, the tricritical point of the first Mott-insulator lobe as obtained by the QMC simulations of Krauth and Trivedi[7] is marked by a solid circle with error bars (the chemical potential for the tip of the Mott lobe was not reported in Ref. 7, and so we fixed it to be μ_{crit}). The solid line is the strong-coupling expansion truncated to third order, while the dotted line is an extrapolation described below. Their simulation gives a critical value of $x_{\mathrm{crit}}=0.122\pm0.006$, whereas our calculation yields $x_{\mathrm{crit}}\approx0.136$ which is in reasonable agreement. Note that the qualitative shape of the Mott lobes has changed from one dimension to two dimensions, mimicking the power-law critical behavior of the XY model in three or larger dimensions.

Figure 2(b) shows the corresponding figure for the $n_0\to\infty$ limit corresponding to the quantum rotor model. The

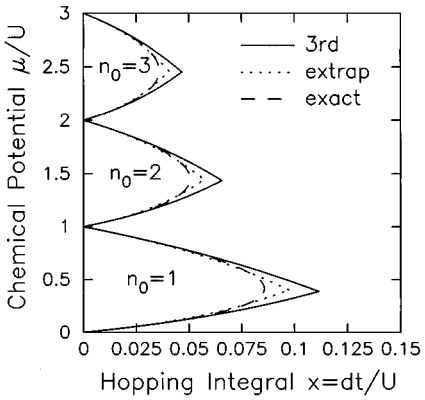

FIG. 3. The x, μ phase diagram of the Bose Hubbard model in infinite dimensions ($d\to\infty$). The solid lines give the phase boundaries of the Mott insulator to the superfluid state as determined from a third-order strong-coupling calculation. The dashed lines are the result of the mean-field calculation of Fisher *et al.* (Ref. 1). The dotted lines are the chemical-potential extrapolation described in the text.

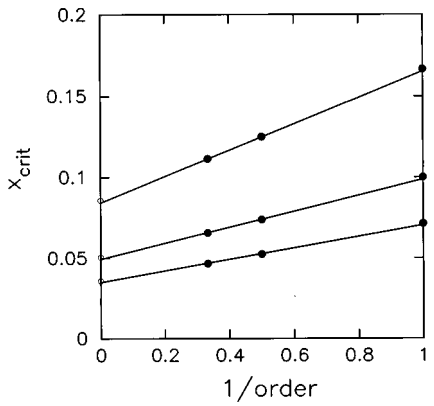

FIG. 4. The critical-point extrapolation method in infinite dimensions. The solid circles are the results for $x_{\rm crit}$ calculated at first, second, and third order. The solid line is the linear extrapolation to infinite order. The open circles are the exact result. Three cases are shown $n_0=1$ (top), $n_0=2$ (middle), and $n_0=3$ (bottom). Note that although the three points have a correlation coefficient larger than 0.9999 the accuracy of the extrapolated critical point is only on the order of 2%.

QMC results are from van Otterlo and Wagenblast.[8] The horizontal axis has been rescaled to $y_\infty=\lim_{n_0\to\infty}n_0x$. We believe that the relatively large difference between the QMC and the strong-coupling perturbation theory arises from the use of the Villain approximation in the QMC simulations.

Finally the strong-coupling expansion is compared to the exact calculation in infinite dimensions.[1] In infinite dimensions, the hopping matrix element must scale inversely with the dimension,[15] $t=t^*/d$, $t^*=$finite, producing the mean-field-theory result of Eq. (13). In Fig. 3 the strong-coupling expansion (solid line) is compared to the exact solution (dashed line) and to an extrapolated solution (dotted line) which will be described below. Even in infinite dimensions, the agreement of the strong-coupling expansion with the exact results is quite good.

As a general rule, the truncated strong-coupling expansions appear to be more accurate in *lower* dimensions, which implies that the density fluctuations of the Bose Hubbard model are also more important in lower dimensions.

At this point we turn our attention to techniques which enable us to extrapolate the strong-coupling expansions to infinite order in hopes of determining a more accurate phase diagram. The simplest method is called critical-point extrapolation. The critical point $(\mu_{\rm crit},x_{\rm crit})$ is calculated at each order (m) of the strong-coupling expansion and is extrapolated to infinite order $(m\to\infty)$. The ansatz that the extrapolation is linear in $1/m$ can be checked by determining the correlation coefficient r of the critical points (a value of $|r|$ that is near 1 indicates a linear correlation). The correlations are found to be most linear for large dimensions ($|r|=0.999\,99$ in infinite dimensions for the first Mott lobe) but remain fairly linear even in one dimension ($|r|>0.995$ for the $x_{\rm crit}$ extrapolation and $|r|>0.95$ for the $\mu_{\rm crit}$ extrapolation). Since the second- and third-order expansions are expected to be more accurate than the first-order calculation, we adopt the following strategy for performing the extrapolations: The results of the second- and third-order expansions are extrapolated to $m\to\infty$ to determine the estimate for the critical point, and the results of the first, second, and third orders are then extrapolated to $m\to\infty$ in order to estimate the error in the critical point and to test the linear-extrapolation hypothesis. The error estimate is chosen to be 1.5 times as large as the difference between the two different extrapolations. Figure 4 plots the critical hopping matrix elements $x_{\rm crit}$ versus $1/m$ for the infinite-dimensional case and $n_0=1,2,3$. The solid dots are the results of the strong-coupling expansion truncated to mth order and the solid line is the linear extrapolant. The open circles are the exact solutions from Eq. (14). Note that although the linear correlation coefficient is very close to 1, the error in the critical point is about 2%. The results for the critical-point extrapolation are recorded in Table I.

The critical-point extrapolation does not yield any information on the shape of the Mott lobes, but only determines the critical point. An alternate extrapolation technique, called the chemical-potential extrapolation method, will determine an extrapolated Mott-phase lobe and critical point. The idea is to fix the magnitude of the hopping matrix elements and determine the value of the chemical potential from Eqs. (11) and (12) for the upper and lower branches of the Mott lobe. The chemical potential is determined from a first-, second-, and third-order calculation and then extrapolated to infinite order assuming the ansatz of a linear dependence upon $1/m$. This procedure determines an extrapolated Mott lobe that should be more accurate than the truncated strong-coupling series. The result for the infinite-dimensional case is presented as a dotted line in Fig. 3. Note that the critical point is not determined as accurately by this technique as it was in the critical-point extrapolation method. The chemical-potential extrapolation method fails in one dimension since the extrapolated branches of the extrapolated Mott lobe do not close.

A third approach is to use the results of the scaling theory.[1] The critical point is that of a $(d+1)$-dimensional XY model, and therefore, has a Kosterlitz-Thouless shape in one dimension and a power-law shape in higher dimensions.

TABLE I. Results for the critical-point extrapolation method described in the text. The critical point is recorded for the first three Mott lobes in one, two, three, and infinite dimensions. Where possible the results from other calculation techniques are displayed in the last column.

Dimension	n_0	$\mu_{\rm crit}$	$x_{\rm crit}$	$x_{\rm crit}$(exact)
1	1	0.255 ± 0.11	0.245 ± 0.012	0.215 ± 0.010[a]
	2	1.359 ± 0.06	0.145 ± 0.009	0.130 ± 0.020[a]
	3	2.400 ± 0.04	0.103 ± 0.006	0.104 ± 0.020[a]
2	1	0.388 ± 0.05	0.114 ± 0.013	0.122 ± 0.006
	2	1.435 ± 0.03	0.067 ± 0.006	
	3	2.454 ± 0.02	0.048 ± 0.004	
3	1	0.400 ± 0.03	0.101 ± 0.008	
	2	1.441 ± 0.02	0.060 ± 0.004	
	3	2.458 ± 0.01	0.042 ± 0.002	
∞	1	0.416 ± 0.001	0.0843 ± 0.001	0.0858
	2	1.451 ± 0.002	0.0494 ± 0.002	0.0505[c]
	3	2.465 ± 0.001	0.0351 ± 0.001	0.0359[c]

[a]Ref. 2 (Monte Carlo simulation at finite temperature).
[b]Ref. 7 (Monte Carlo simulation at finite temperature).
[c]Ref. 1 [exact solution from Eq. (14)].

Examination of the exact result for infinite dimensions (13) leads one to propose the following ansatz for the Mott lobe in $d\geq 2$:

$$\frac{\mu}{U}-n_0=A(x)\pm B(x)(x_{\rm crit}-x)^{z\nu}, \tag{15}$$

where $A(x)\equiv a+bx+cx^2+\cdots$ and $B(x)\equiv\alpha+\beta x+\gamma x^2+\cdots$ are regular functions of x (which should be accurately approximated by their power-series expansions) and $z\nu$ is the critical exponent for the $(d+1)$-dimensional XY model. In the unconstrained-scaling-analysis extrapolation method the exponent $z\nu$ is determined by the strong-coupling expansion in addition to the parameters a,b,c and α,β,γ. This provides a perturbative estimate of the exponent $z\nu$ which can be checked against its well-known values. In the constrained-scaling-analysis extrapolation method $z\nu$ is fixed at its predicted values[1] of $z\nu\approx 2/3$ in two dimensions and $z\nu=0.5$ in higher dimensions. In direct analogy to Eq. (15), we propose the Kosterlitz-Thouless form

$$\frac{\mu}{U}-n_0=A(x)\pm B(x)\exp\left[-\frac{W}{\sqrt{x_{\rm crit}-x}}\right] \tag{16}$$

for the constrained-extrapolation-method in one dimension.

When the unconstrained-scaling-analysis extrapolation method is carried out, one finds that there is no solution for the critical exponent in one dimension (which is consistent with Kosterlitz-Thouless behavior), that in $d=2$ the exponent satisfies $z\nu\approx 0.58$, in $d=3$ the exponent is $z\nu\approx 0.54$, and in infinite dimensions $z\nu\approx 0.5$. There is a slight n_0 dependence to the exponents that are calculated in this method, but that arises from the truncation of the series to such a low order. In general, the unconstrained-extrapolation method produces an accuracy of about 15% in the exponent $z\nu$, and the method appears to work best in higher dimensions.

The results for the constrained-extrapolation method are plotted with a dotted line in Fig. 1 for the one-dimensional case. The values of the critical points are ($\mu_{\rm crit}=0.186$, $x_{\rm crit}=0.265$), (1.319,0.155), and (2.371,0.111) for $n_0=1$, 2, and 3, respectively. These critical points occur at larger values of x than predicted by the QMC simulations,[2] but it is difficult to gauge whether the extrapolated series expansions are more or less accurate than the QMC simulations because of the finite-temperature effects in the latter. The constrained-extrapolation results in two dimensions are plotted with a dotted line in Figs. 2(a) and 2(b). The values of the critical points are (0.375,0.117), (1.426,0.069), and (2.448,0.049) for $n_0=1$, 2, and 3, respectively. The agreement with the QMC simulations[7] is excellent. Similarly, the extrapolated critical point for the $2-d$ rotor model is (0.5,0.171) which also agrees well with the QMC. In this latter case [Fig. 2(b)] the errors between the extrapolated series expansion and the QMC can be traced to the use of the Villain approximation in the latter. When the constrained-scaling-analysis extrapolation method is applied to the infinite-dimensional case the result is indistinguishable from the exact solution when the two are plotted on the same graph.

The extrapolation techniques work best in *higher* dimensions, virtually producing the exact result in infinite dimensions. This gives us confidence that the extrapolated results of the series expansions can produce numerical answers that are at least as accurate as the QMC simulations.

III. DISORDERED CASE

The most common type of disorder distribution that has been considered in relationship to the ''dirty'' boson problem is the Anderson model (continuous disorder distribution). In the Anderson model the distribution $\rho(\epsilon)$ for the on-site energies $\{\epsilon_i\}$ is continuous and flat, satisfying

$$\rho(\epsilon)=\theta(\Delta-\epsilon)\,\theta(\Delta+\epsilon)\,\frac{1}{2\Delta}. \tag{17}$$

The symbol Δ denotes the maximum absolute value that the site energy ϵ_i can assume for a given (bounded) distribution ($|\epsilon_i|\leq\Delta U$). This disorder distribution is symmetric

$[\rho(-\epsilon)=\rho(\epsilon)]$ and in particular it satisfies $\Sigma_i \epsilon_i = 0$. The results presented in this contribution are *insensitive* to the actual shape of the disorder distribution; all we require is a symmetric distribution with $|\epsilon_i| \leq \Delta U$.

We begin by reexamining the exact solution of the infinite-range-hopping model.[1] If all energies are measured in units of the boson-boson repulsion U, then the analysis of Ref. 1 derives an equation that relates the hopping matrix elements to the chemical potential at the Mott-phase boundary:

$$\frac{1}{2x} = \int_{-\infty}^{\infty} \left[-\frac{n_0+1}{y+\epsilon} + \frac{n_0}{y+1+\epsilon} \right] \rho(\epsilon) d\epsilon, \qquad (18)$$

with $y \equiv -n_0 + \mu/U$ the chemical potential and $\rho(\epsilon)$ the disorder distribution. This solution assumes that the phase transition from the Mott phase to the Bose glass is a *second-order* phase transition.

When Eq. (18) is solved for the Anderson model distribution (17), one finds that the chemical potential for the lower branches of the Mott lobe behaves like $y = -\Delta - \exp[-1/2x(n_0+1)]$ for small x. This result is *nonperturbative* in the hopping matrix elements and cannot be represented by a simple perturbative theory about $x=0$. The reason why this happens is that the infinite-range-hopping model has no localized states for any disorder distribution (however, this statement does depend on the disorder distribution[16]). Localized states can occur in the infinite-dimensional limit at the tails of the distribution. Therefore we expect that the transition will have a different qualitative character on a hypercubic lattice with nearest-neighbor interactions. In fact, the perturbative arguments given in the Introduction show that the phase boundaries have the *same* slope as they did in the pure case. Furthermore, we expect the transition to be first order at the tip of the Mott lobe because the states that the bosons initially occupy in the compressible phase are localized within the rare regions of the lattice (where the site energies are all equal to $-\Delta U$), implying that there is no diverging length scale at the transition. The perturbative expansion for the energy of the Mott phase is unchanged from Eq. (8) in the presence of disorder (if the disorder distribution satisfies $\Sigma_i \epsilon_i = 0$), while the defect phases have a trivial dependence upon disorder (in the thermodynamic limit)—the energy for a particle or hole defect state is shifted by $-\Delta U$, and so the effect of the disorder is simply to shift the Mott-phase boundaries inward by ΔU. The critical point, where the Mott phase disappears, is no longer described by a second-order critical point [in which the slope of $\mu(x)$ becomes infinite at $x_{\rm crit}$] but rather is described by a first-order critical point [in which the slope of $\mu(x)$ changes discontinuously at $x_{\rm crit}$].

In the thermodynamic limit one can always find a rare region of arbitrarily large extent which guarantees the existence of the first-order transition, but the density of these rare regions is an exponentially small function of their size. For this reason the compressibility at the Mott-phase boundary will also be exponentially small. Finite-size effects play a much more important role in the disordered case: *It is impossible to determine the Mott-phase boundary accurately in the thermodynamic limit by scaling calculations performed on small lattices, because the lattice size must be large enough to contain rare regions within which the bosons can be delocalized.* (Finite-size effects can be studied with the strong-coupling expansion which is given to third order in the single-particle matrix S in the Appendix.)

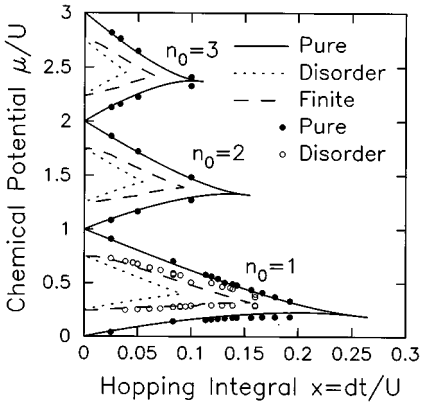

FIG. 5. Phase diagram in one dimension with disorder. The perturbative approximations are plotted with solid (dotted) lines for the pure (disordered) cases in the thermodynamic limit. Three cases of disorder are included: $(\Delta = 0.125, 0.25, 0.375)$. The dashed line is the perturbative results for a finite system with 256 lattice sites. The solid dots are the quantum Monte Carlo results from Ref. 2 in the pure case, and the open dots are for the disordered case with $\Delta = 0.25$ (the disordered calculations were performed on lattice sizes ranging from 16 to 256 sites).

The most accurate way of calculating the Mott-phase boundary is then to take the results of the constrained-scaling-analysis extrapolation for the pure case and shift the branches by the strength of the disorder. This is plotted in Fig. 5 for the one-dimensional case and two different values of disorder $(\Delta = 0, 0.25)$. The thermodynamic limit is represented by the solid line for the pure case and dotted lines for the disordered case, while the dashed line is the result of an Anderson-model disorder distribution on a finite lattice with 256 sites. The QMC results of Scalettar and co-workers[2] correspond to lattice sizes ranging from 16 sites to 256 sites (the disorder parameter is $\Delta = 0$ for the solid dots and $\Delta = 0.25$ for the open dots). The Mott phase is stabilized on finite-sized systems because they do not possess the rare regions needed to correctly determine the Mott-phase boundary. This is clearly seen in the QMC results, which predict a much larger region for the Mott phase than strong-coupling perturbation theory does in the thermodynamic limit. The perturbative results for a finite system are much closer to the QMC results as expected. (Note that the finite-size calculations have not been extrapolated, and so they should underestimate the stability of the Mott phase in one dimension which is clearly seen in Fig. 5.) Also the slope of the phase boundary approaches zero (as $x \to 0$) for the finite-size systems.[2]

Figure 6 plots the Mott-phase diagram for the disordered Bose Hubbard model in two dimensions and one value of the disorder $(\Delta = 0, 0.182)$ in the thermodynamic limit. The solid dot (with error bars) is the QMC result[7] (for the pure case with $\Delta = 0$) and the open dot is the disordered case $(\Delta = 0.182)$. Note that in dimensions larger than one, the finite-size effects for the tip of the Mott lobe are not as strong as they are in one dimension.

We compare in Fig. 7 the differences between the infinite-

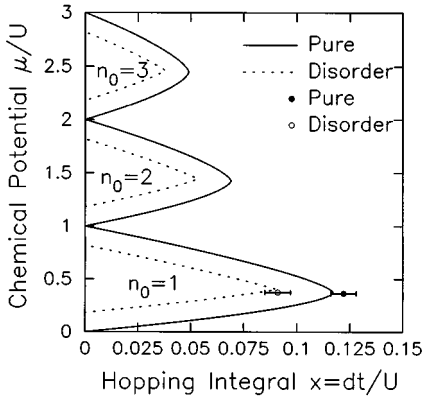

FIG. 6. Phase diagram in two dimensions with disorder. The perturbative approximations are plotted with solid (dotted) lines for the pure (disordered) cases in the thermodynamic limit. The disorder was set equal to $\Delta = 0.182$. The solid (open) dots are the quantum Monte Carlo results of Ref. 7 for the pure (disordered) cases. Surprisingly, in two and higher dimensions, the finite-size effects in the disordered regime appear to be weaker.

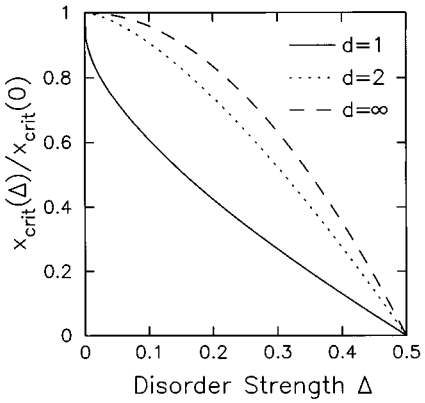

FIG. 8. Plot of $x_{\mathrm{crit}}(\Delta)/x_{\mathrm{crit}}(0)$ as a function of dimension. The solid line is for one dimension, the dotted line for two dimensions, and the dashed line for infinite dimensions. Note that the intitial decrease of x_{crit} is very rapid in one dimension, because of the cusplike shape of the Mott lobe in the pure case, but is much slower in higher dimensions (because the tip has a power-law behavior in the pure case).

dimensional lattice and the infinite-range-hopping model of Ref. 1. The solid lines correspond to the exact solution with no disorder, the dotted lines are the infinite-dimensional lattice strong-coupling expansion with disorder ($\Delta = 0.2$), and the dashed lines are the exact solution of the infinite-range-hopping model. In the case of disorder, the first-order nature of the transition is evidenced by the jump in the slope of the Mott phase boundary at the tip of the lobe. The second-order phase boundaries predict a more stable Mott phase, and their slopes all approach zero as $x \to 0$. We expect in the region in between the (first-order) infinite-dimensional phase boundary and that of the (second-order) infinite-range-hopping model that the compressibility will be exponentially small, and will only become sizable as the second-order phase boundary is crossed.

Because the Mott-phase to Bose-glass phase transition is first order for the disordered case, and since the Bose-glass to superfluid transition is always second order (because it involves a collective excitation that extends through the entire lattice), it is quite unlikely that there would ever be a region where the Mott phase has a transition directly to the superfluid. *The presence of the Lifshitz rare regions strongly supports the picture that the Mott phase is entirely enclosed within the Bose-glass phase.* This result is *independent* of any perturbative arguments, since the rare regions must dominate the Mott to Bose-glass transition in the exact solution too.

Finally, we calculate the dependence of the critical value of x at the tip of the Mott-phase lobe, as a function of the disorder strength Δ. Figure 8 plots this value of $x_{\mathrm{crit}}(\Delta)/x_{\mathrm{crit}}(0)$ versus Δ for the one-, two-, and infinite-dimensional cases. The plot is limited to the lowest Mott-phase lobe with $n_0 = 1$. Since the one-dimensional Mott phase lobes have a cusplike behavior that is removed when disorder is added to the system, we expect x_{crit} to decrease very rapidly for small disorder. This effect is sharply reduced in higher dimensions. In the strong-disorder limit, the phase diagram is dominated by the first-order terms in the perturbative expansion, which have a trivial dependence on the dimensionality, but the slopes of the curves are unequal because $x_{\mathrm{crit}}(0)$ depends strongly upon the dimensionality.

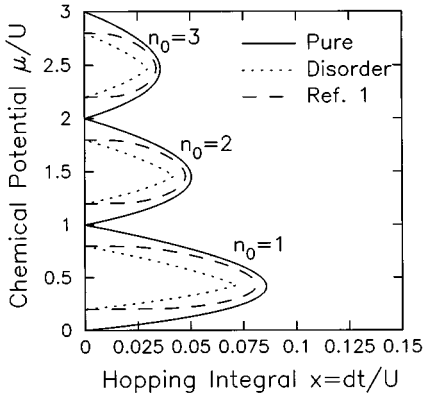

FIG. 7. Phase diagram in infinite dimensions with disorder. The perturbative approximations are plotted with solid (dotted) lines for the pure (disordered) cases in the thermodynamic limit. The disorder was set equal to $\Delta = 0.2$. The dashed line is the exact solution of the infinite-range-hopping model from Ref. 1. Note how the Mott phase is more stable with the infinite-range calculation, and how it has vanishing slope as $x \to 0$. Interestingly, the location of the tip of the Mott lobe is close for both the infinite-dimensional and the infinite-range calculations.

IV. CONCLUSION

We have developed a strong-coupling perturbation-theory approximation to the Bose-Hubbard model on a bipartite lattice. The perturbative results can be extrapolated in a number of different ways which either do or do not take into account the scaling theory of the critical point at the Mott tip. We find that a perturbative expansion through third order rivals the accuracy of the QMC simulations, and is likely the best method for determining the Mott-phase boundary of these interacting Bose systems.

We treated two different cases: the pure case and the disordered case. In the pure case the tip of the Mott lobe satis-

fies a scaling relation because it corresponds to a second-order phase transition in a $(d+1)$-dimensional XY model. This is because the compressible phase is also superfluid which implies there is a diverging length scale at the phase transition. Calculations in the pure case are insensitive to finite-size effects. In the disordered case we argued that the tip of the Mott-phase lobe corresopnds to a first-order phase transition because the initial single-particle excitations are localized into the rare regions of the Lifshitz tails for any bounded disorder distribution. As a result there is a kink in the Mott-phase boundary since the slope of $\mu(x)$ has a discontinuous jump at the tip of the lobe. In this case, there are strong finite-size effects because ''typical'' disorder distributions on finite lattices do not have Lifshitz tails.

The results of these perturbative calculations have been compared to the available QMC simulations. We find a remarkable agreement between the two and are unable to determine which method is more accurate in a quantitative determination of the phase boundaries.

The perturbation theory described here falls short in one aspect—it is unable to determine the Bose-glass–superfluid phase transition in the disordered case. It is possible that such a calculation could be performed, but since the particle density at which it occurs is *a priori* not known, and since the superfluid susceptibility diverges in the Bose-glass phase, such a calculation may be problematic.

ACKNOWLEDGMENTS

We would like to thank M. Fisher, Th. Giamarchi, M. Jarrell, M. Ma, A. van Otterlo, R. Scalettar, R. Singh, and G. Zimanyi for many useful discussions. We would especially like to thank M. Ma for pointing out that the Mott to Bose-glass phase transition is first order in the disordered case. Initial stages of this work were carried out by J.K.F. at the University of California, Davis in 1994 and were completed during a visit to l'École Polytechnique Fédérale de Lausanne in June 1995. J.K.F. would like to thank the Office of Naval Research (under Grant No. N00014-93-1-0495) for support while at UC Davis, and would like to thank the Donors of the Petroleum Research Fund, administered by the American Chemical Society (ACS-PRF-29623-GB6) for support while at Georgetown.

APPENDIX: FINITE-SIZE EFFECTS FOR THE DISORDERED CASE

The Rayleigh-Schrödinger perturbation theory for the case with disorder is straightforward, but rather tedious. In the thermodynamic limit, the perturbative expansion simplifies because it is dominated by the rare regions of the lattice. For a finite-sized system, the perturbative results are more complicated. We summarize here the main results for a third-order strong-coupling expansion in the presence of disorder.

The only assumptions that are made about the disorder distribution is that it is bounded and symmetric, so that $|\epsilon_i| \leq \Delta U$ and $\Sigma_i \epsilon_i = 0$. Restriction is also made to bipartite lattices.

The upper phase boundary for the Mott to Bose-glass transition is found by solving the equation

$$\delta^{(\mathrm{part})}(n_0) = \frac{\Lambda}{U}(n_0+1) + \frac{1}{2}\frac{Zt^2}{U^2} n_0(5n_0+4) - \sum_{ijk} f_i \frac{t_{ij}t_{jk}}{U^2} f_k n_0(n_0+1) - n_0(n_0+1)\Bigg[\sum_{ijkl} f_i \frac{t_{ij}t_{jk}t_{kl}}{U^3} f_l (3n_0+2)$$

$$+ \frac{\Lambda}{U}\sum_{ijk} f_i \frac{t_{ij}t_{jk}}{U^2} f_k (n_0+1) - \frac{Zt^2}{U^2}\sum_{ij} f_i \frac{t_{ij}}{U} f_j (9n_0+6) + \frac{t^2}{U^2}\sum_{ij} f_i \frac{t_{ij}}{U} f_j (4n_0+2) - \frac{\Lambda Z t^2}{U^3}\left(\frac{11}{4}n_0 + \frac{5}{2}\right)$$

$$- \sum_{ijk} \frac{(\epsilon_i - \epsilon_j + \epsilon_k)}{U} f_i \frac{t_{ij}t_{jk}}{U^2} f_k \Bigg] + n_0 \Bigg[\sum_{ij} \frac{\epsilon_i}{U}\frac{t_{ij}^2}{U^2} f_j^2 \left(\frac{3}{2}n_0 + 2\right) - \frac{Zt^2}{U^2}\sum_i \frac{\epsilon_i}{U} f_i^2 \left(\frac{17}{4}n_0 + \frac{9}{2}\right)\Bigg], \tag{A1}$$

where f_i is the minimal eigenvector of the single-particle matrix $S_{ij}^{(\mathrm{part})} = -t_{ij} + \epsilon_i \delta_{ij}/(n_0+1)$ and Λ is its corresponding eigenvalue. The identity $\Sigma_{ij} t_{ij}^2 f_j^2 = Zt^2$ was needed in deriving the above result. A similar calculation yields

$$\delta^{(\mathrm{hole})}(n_0) = -\frac{\tilde{\Lambda}}{U} n_0 - \frac{1}{2}\frac{Zt^2}{U^2}(n_0+1)(5n_0+1) + \sum_{ijk} g_i \frac{t_{ij}t_{jk}}{U^2} g_k n_0(n_0+1) - n_0(n_0+1)\Bigg[-\sum_{ijkl} g_i \frac{t_{ij}t_{jk}t_{kl}}{U^3} g_l (3n_0+1)$$

$$- \frac{\tilde{\Lambda}}{U}\sum_{ijk} g_i \frac{t_{ij}t_{jk}}{U^2} g_k n_0 + \frac{Zt^2}{U^2}\sum_{ij} g_i \frac{t_{ij}}{U} g_j (9n_0+3) - \frac{t^2}{U^2}\sum_{ij} g_i \frac{t_{ij}}{U} g_j (4n_0+2) + \frac{\tilde{\Lambda} Z t^2}{U^3}\left(\frac{11}{4}n_0 + \frac{1}{4}\right)$$

$$- \sum_{ijk} \frac{(\epsilon_i - \epsilon_j + \epsilon_k)}{U} g_i \frac{t_{ij}t_{jk}}{U^2} g_k \Bigg] + (n_0+1)\Bigg[\sum_{ij} \frac{\epsilon_i}{U}\frac{t_{ij}^2}{U^2} g_j^2 \left(\frac{3}{4}n_0 + \frac{1}{4}\right) - \frac{Zt^2}{U^2}\sum_i \frac{\epsilon_i}{U} g_i^2 \left(\frac{7}{2}n_0 + \frac{1}{2}\right)\Bigg] \tag{A2}$$

for the lower phase boundary of the Mott to Bose-glass transition. Here we have that g_i is the minimal eigenvector of the single-particle matrix $S_{ij}^{(\mathrm{hole})}=-t_{ij}-\epsilon_i\delta_{ij}/n_0$ and $\tilde{\Lambda}$ is its corresponding eigenvalue.

In the thermodynamic limit we know that the minimal eigenvalue occurs in the rare regions where the disorder is constant and equal to its extreme value. The ground-state eigenvector is delocalized within the rare region (to minimize its kinetic energy) and localized to the rare region (to minimize its disorder energy). Such an eigenvector is now *separately* an eigenvector of the kinetic-energy matrix and of the disorder matrix, and so we have $-\Sigma_{ij}t_{ij}f_j=\lambda f_i$, $\Sigma_j\epsilon_i\delta_{ij}f_j=-\Delta U f_i$, and $\Lambda=\lambda-\Delta U/(n_0+1)$ with similar formulas for the g eigenvector. Plugging these thermodynamic limits into Eqs. (A1) and (A2) then yields the result that the Mott-phase boundaries are only shifted uniformly by ΔU, and all higher-order dependence on the disorder vanishes.

[1] M. P. A. Fisher, P. B. Weichman, G. Grinstein, and D. S. Fisher, Phys. Rev. B **40**, 546 (1989).

[2] R. T. Scalettar, G. G. Batrouni, and G. T. Zimanyi, Phys. Rev. Lett. **66**, 3144 (1991); P. Niyaz, R. T. Scalettar, C. Y. Fong, and G. G Batrouni, Phys. Rev. B **44**, 7143 (1991); G. G. Batrouni and R. T. Scalettar, *ibid.* **46**, 9051 (1992).

[3] D. S. Rokhsar and B. G. Kotliar, Phys. Rev. B **44**, 10328 (1991); K. G. Singh and D. S. Rokhsar, *ibid.* **46**, 3002 (1992).

[4] E. S. Sörensen, M. Wallin, S. M. Girvin, and A. P. Young, Phys. Rev. Lett. **69**, 828 (1992).

[5] A. P. Kampf and G. T. Zimanyi, Phys. Rev. B **47**, 279 (1993); C. Bruder, R. Fazio, A. Kampf, A. van Otterlo, and G. Schön, Phys. Scr. **42**, 159 (1992); C. Bruder, R. Fazio, and G. Schön, Phys. Rev. B **47**, 342 (1993).

[6] W. Krauth, M. Caffarel, and J. P. Bouchaud, Phys. Rev. B **45**, 3137 (1992); K. Sheshadri, H. R. Krishnamurty, R. Pandit, and T. V. Ramkrishnan, Europhys. Lett. **22**, 257 (1993).

[7] W. Krauth and N. Trivedi, Europhys. Lett. **14**, 627 (1991); W. Krauth, N. Trivedi, and D. Ceperley, Phys. Rev. Lett. **67**, 2307 (1991).

[8] A. van Otterlo and K.-H. Wagenblast, Phys. Rev. Lett. **72**, 3598 (1994); (unpublished).

[9] G. G. Batrouni, R. T. Scalettar, G. T. Zimanyi, and A. P. Kampf, Phys. Rev. Lett. **74**, 2527 (1995).

[10] J. K. Freericks and H. Monien, Europhys. Lett. **24**, 545 (1994); H. Monien and J. K. Freericks, in *Strongly Correlated Electronic Materials*, edited by K. S. Bedell, Z. Wang, D. E. Meltzer, A. V. Balatsky, and E. Abrahams (Addison-Wesley, Reading, MA, 1994), p. 320.

[11] T. Giamarchi and H. J. Schulz, Phys. Rev. B **37**, 325 (1988).

[12] M. Ma, B. I. Halperin, and P. A. Lee, Phys. Rev. B **34**, 3136 (1986).

[13] I. M. Lifshitz, Sov. Phys. Usp. **7,** 549 (1965); F. Cyrot-Lackmann, J. Phys. C **5,** 300 (1972).

[14] R. Scalettar (private communication).

[15] E. Müller-Hartmann, Int. J. Mod. Phys. B **3**, 2169 (1989).

[16] F. Pázmándi, G. Zimányi, and R. Scalettar, Phys. Rev. Lett. **75**, 1356 (1995).